Available online at www.sciencedirect.com

ScienceDirect

Procedia Engineering 88 (2014) 117 – 124

Procedia Engineering

www.elsevier.com/locate/procedia

International Symposium on Dynamic Response and Failure of Composite Materials, DRaF2014

A Repair Criterion for Impacted Composite Structures Based on the Prediction of the Residual Compressive Strength

R. Borrelli[a*], S. Franchitti[a], F. Di Caprio[a], U. Mercurio[a,b], A. Zallo[c]

[a]*CIRA S.C.p.A. – Centro Italiano Ricerche Aerospaziali, 81043 Capua (CE), Italy*
[b]*IMAST S.c.a.r.l. – Technological District on Engineering of Polymeric and Composite Materials and Structures, 80055 Portici (NA), Italy*
[c]*AVIO S.p.A. 00034 Colleferro (RM), Italy*

Abstract

The residual strength in particular the compression strength after damages due to low velocity impact is one of the most critical issue for composite laminates. If the impact event induces relevant damages on composite components, a repair of the degraded parts is necessary. The aim of this work is to develop a repair criterion to be applied on the composite structures of the European launch vehicle VEGA. The criterion is based on a numerical procedure which was validated in a previous research work and which allows to predict the impact damage and the post impact residual strength as function of the impact energy, making possible to determine the energy threshold beyond which it is necessary to repair the component.

Peer-review under responsibility of the Organizing Committee of DRaF2014

Keywords: Composite damage, residual strength, virtual CAI, LS-Dyna, ANSYS®

1. Introduction

Fiber-reinforced polymer composites, especially CFRP, are very susceptible to reductions in strength due to accidental impact damage. For compression loaded structures, such reduction in strength can be important and it is typically accounted for in design through the use of conservative material design allowable. Composite structures impacted and damaged during maintenance or handling operations become production rejects resulting in huge economic losses. For these reasons, the definition and the validation of a repair methodology is a task of primary interest for composite manufacturers.

The aim of this work is to develop a repair criterion to be applied on the composite structures of the European launch vehicle VEGA. VEGA is a four stages vehicle; the first three stages (P80, Zefiro23 and Zefiro9) are powered

* Corresponding author. Tel.: +39-0823-62-3544; fax: +39-0823-62-3515.
E-mail address: r.borrelli@cira.it

Peer-review under responsibility of the Organizing Committee of DRaF2014
doi:10.1016/j.proeng.2014.11.134

by one Solid Rocket Motor (SRM) which is typically a filament winding cylindrical composite case with closed dome. Each case is supplied with a forward and aft ward skirt which assures stages connection (Fig. 1).

Fig. 1: Typical lay-out of VEGA SRM

The impact risk analysis starting from the manufacturing activity (composite case production) up to the final assembly revealed that, from an impact threat point of view, the most critical parts of the launch vehicle are the skirts. The skirts, which have the purpose of supporting the flight loads transmitted from the engine to the rest of the launcher, are mainly subject to compressive loads. Given such state of stress and given the large radii of curvature of the skirts it is reasonable to investigate the impact and post-impact behavior of these parts assimilating them to standardized Compression After Impact (CAI) 100 x 150 mm flat specimens.

The repair criterion proposed in this work has been applied on CAI specimens representative of the skirt parts of the three stages that constitute the launch vehicle. The criterion is based on the numerical procedure which allows to predict the impact damage and the post impact residual strength. Such research activity was developed within the context of the project PRADE, funded by the Italian Ministry of University and Research (MIUR).

2. Literature

In the past, a lot of effort has been spent on the prediction of the impact damage and residual strength of impacted composite structures. Abrate gives a good overview of impact studies on composite materials in his book [1] and his survey papers [2], [3]. Considerable experimental studies [4] - [9] have been devoted to the problem with the aim of improving impact tolerance and investigating sensibility to stacking sequences, thickness, impact location, resin and fiber properties. The use of composites in the manufacture of cryogenic fuel tanks for future reusable launch space vehicles was the motivation for the study performed in [10] on the CAI performance at low temperature of composite laminates subjected to low-velocity impact.

At each step of the certification process of composite structural components, a combination of testing and analysis techniques is typically performed [11] since only the testing can be prohibitively expensive due to the large number of specimens needed to verify every geometry, loading, environment and failure mode. Therefore developments of reliable analysis tools for the prediction of both the impact response and the residual strength are very important in order to assess and improve structures.

In literature the prediction of residual strength of composite structures is approached in different ways.

The difficulties in facing this kind of problem, from a numerical point of view, stay in the fact that the prediction of the impact response and the prediction of its evolution under the service loads belong to two different disciplines. Such disciplines are usually indicated with the terms “damage resistance” and “damage tolerance” and have historically travelled independently to each other: the impact event is a dynamic one and it is better simulated by using FE code based on explicit time integration scheme. On the other hands, service loads are usually applied in a quasi-static way making the use of implicit code more appropriate. For these reasons, many authors proposed to predict the residual strength of impacted composite laminates by replacing the real and complex impact damage with a simpler “artificial” equivalent damage like delamination [12] - [14] or open hole [15], [16]. Thus, the damage tolerance of the structure is investigated by including these equivalent defects in a simulation approach for determining the residual strength.

Only in a few works [17] - [20], the complete process (two-step simulation) of both impact simulation and residual compression strength simulation is presented. In these works, the post-impact residual behavior is investigated by using the same explicit code employed to study the impact response even if the applied loads are applied in a quasi-static mode.

In [21], a numerical procedure for the virtual compression after impact analysis was proposed and validated against experimental results. The repair criterion proposed in the present work is based on such numerical procedure which was applied to CAI specimens representative of the skirt parts of the three stages that constitute the launch vehicle. The numerical procedure allows to compute the loss of compressive strength as function of the impact energy and damaged area extension, making possible to determine the energy threshold or in alternative the damaged area limit beyond which it is necessary to repair the component.

3. Virtual procedure applied on CAI specimens representative of the skirt parts of the launch vehicle VEGA

In this work, the numerical procedure of VIRTUAL CAI, proposed in detail in [21], was applied to CAI specimens representative of the skirt parts of the three stages that constitute the launch vehicle (P80, Zefiro23 e Zefiro9).

The scope of this procedure is to estimate the residual strength of a laminate through two separate steps:

- To simulate the drop-weight impact test, aimed at inducing damage into the composite laminates, by using the commercial explicit code LS-Dyna;
- To simulate the compression after impact test, determining the residual compression strength, by using the commercial implicit code ANSYS®.

The second stage in the approach uses the impact damage distribution which is transferred to the implicit code by a macro written by using the ANSYS® Parametric Design Language (APDL).

3.1. Impact analysis

A sketch of the specimen and of the impact test configuration, according to the standard regulation [22], is shown in Fig. 2 a). Four rubber-tipped clamps restrain the specimen over a rigid fixture base and an hemispherical impactor drops vertically with a certain impact energy.

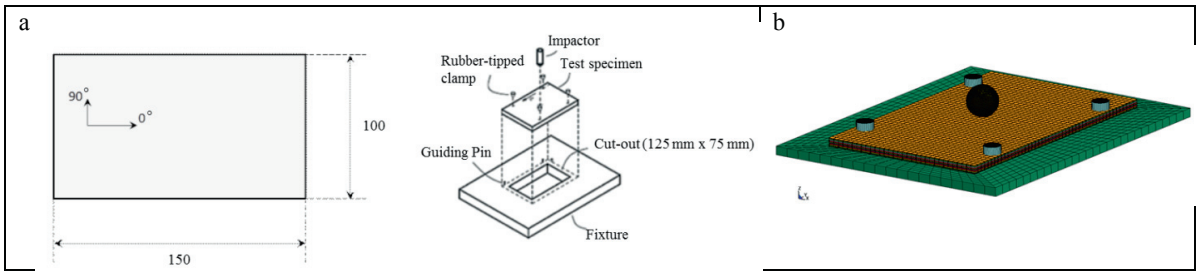

Fig. 2: (a) Specimen dimensions (mm) and sketch of the impact test; (b) LS-Dyna FE model

The FE model, developed in LS-Dyna for the simulation of the impact test, is shown in Fig.2b) and it was a result of an investigation presented in [24] aimed at tuning a FE model reproducing the impact response of a composite laminate.

As the plate length and width dimensions are large compared to the thickness, a 2D modelling approach was chosen. In particular layered fully integrated shell elements with an element length of 3.125 mm were used.

The linear-elastic composite material model MAT54, available in the LS-Dyna library, was adopted to take into account for intralaminar damage (fibre and matrix failures) onset. The progressive failure analysis capability of

MAT54 is based on the Chang-Chang failure criteria [25] which distinguishes between tensile fiber failure, compressive fiber failure, tensile matrix failure and compressive matrix failure. The elastic material behavior of the individual ply is calculated based on the input of the Young's modulus, shear modulus and Poisson's ratio.
The separation of adjacent plies due to normal or shear loads, referred to as delamination, absorbs impact energy and decreases the laminate stiffness and therefore needs to be covered by the model as well. Because delaminations cannot be represented inside the continuum shell elements, the laminate was divided into a certain number of sublaminates with tiebreack contacts in-between, which can fail during the simulation according to a specified failure law. The criterion chosen to describe the phenomenon in the most realistic way consists in modeling adjacent plies, with a difference in orientation lower than 90°, grouped into a unique layer of shell elements; on the other hands, adjacent plies with a difference in orientation equal to 90°, that is where delamination is most likely to occur, were separated by tiebreack contact definition (option 8).
Each stage was simulated considering the symmetric and balanced skirt lay-up; the material used and the number of layers of the shell of the corresponding FE model are summarized in table 1.

Table 1: Materials and FE model for each stage of launch vehicle VEGA

STAGE	MATERIALS		FE MODEL
	TAPE	TOW	
SRM P80	INTERMEDIATE STRENGTH	INTERMEDIATE STRENGTH	19L
SRM Zefiro23	INTERMEDIATE STRENGTH	HIGH STRENGTH	19L
SRM Zefiro9	INTERMEDIATE STRENGTH	HIGH STRENGTH	15L

The fixture support and the hemispherical impactor were defined as rigid bodies since they are stiff steel parts whose stresses and strains distribution are not of interest. In order to capture the effect of the impactor drop, the impactor was modeled just before the impact position by specifying an initial impact velocity, chosen in function of the impact energy to be achieved. A very fine mesh was adopted for the impactor in order to correctly compute the contact force between the impactor and the plate. An automatic surface-to-surface contact based on the standard penalty formulation was defined between the composite plate and the rigid impactor. The presence of the four rubber-tipped clamps was taken into account into the model by constraining the out-of-plane displacement of the nodes belonging to the upper layer of the specimen and positioned under the clamps as shown in Fig. 2b. In order to avoid lability and enforce the symmetry in the mechanical behavior, the *x*-displacement was constrained for the nodes at the centre of the short edges, while the *y*-displacement was constrained for the nodes at the centre of the long edges.
The numerical results of the impact analysis are given in terms of force, impactor displacement and absorbed energy time histories, the contact force vs. impactor displacement curve and the map of the total damage.
The numerical damage was computed by a macro written by using the ANSYS® Parametric Design Language (APDL) which checks the damage variable of each failure mode (fiber tensile, fiber compression, matrix tensile and matrix compression) for all the integration points through the thickness of each finite element. If failure is found the element is plotted in red, intact element are plotted in gray. The macro allows also to map the intralaminar damage distribution in each sublaminate.

3.2. Damage transfer procedure

The damage distribution induced by the impact analysis should be transferred to the ANSYS® model for the subsequent compression after impact analysis. To this aim, another subroutine written in APDL was developed. Such subroutine receives in input the impact damage information which are mapped in a monolayer layered shell ANSYS® model (one layer of shell through the thickness) for the compression analysis. Hence, the damage status generated by the impact event in a certain area of the specimen is taken into account by using degraded material properties in that zone.

3.3. Compression after impact analysis

The compression after impact test was performed, according to the standard regulation [23], under displacement control. The compression load was applied on the shortest edge of the specimen, along the direction of the largest dimension that is the 0° laminate direction. In Fig. 3a) the anti-buckling device is shown. As prescribed by the standard regulation, such device is used to avoid the onset of instability, thus, a pure compression failure was guaranteed.

The 4-node structural layered shell element "shell181", available in the ANSYS® library [26], was used for the compression analysis. The FEM is shown in Fig. 3b) where red elements are associated to a degraded material model. In order to simulate the real boundary conditions experienced during the experimental test, the following constraints were applied:

- $u_y=u_z=rot_x=0$ for all the nodes belonging to the edge AB. Moreover, for the central node of this edge, also ux was set to zero.
- $u_z=rot_y=0$ for all the nodes belonging to the edges BC and AD
- $u_z=rot_x=0$ and u_y=-1.5 mm for all the nodes belonging to the edge CD. Moreover, for the central node of this edge, also ux was set to zero.

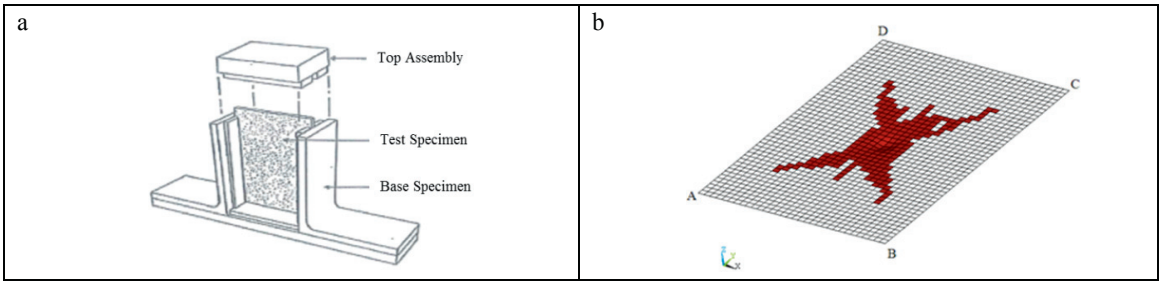

Fig. 3: (a) Sketch of the CAI test according to the ASTM D7137; (b) ANSYS FE model for compression after impact analysis

Once transferred the impact damage status to the ANSYS® FE model, the CAI analysis was performed by using the progressive failure analysis ANSYS® capability.

The numerical result of the compression after impact test is the reaction vs. applied strain curve.

4. Numerical test matrix

Table 2 summarizes the numerical test matrix chosen for the CAI specimens representative of the skirt parts of the three stages that constitute the launch vehicle VEGA.

In particular, five energy levels were fixed (15 J, 25 J, 50 J, 100 J e 150 J) and two impactors with different shape (hemispherical and flat) were investigated; the geometry of the impactors were provided by AVIO [27] and are shown in Fig. 4.

Table 2: Numerical test matrix

	IMPACTOR SHAPE	ENERGY LEVELS [J]
SRM P80	hemispherical	15-25-50-100-150
	flat	15-25-50-100-150
SRM Zefiro23	hemispherical	15-25-50-100-150
	flat	15-25-50-100-150
SRM Zefiro9	hemispherical	15-25-50-100-150
	flat	15-25-50-100-150

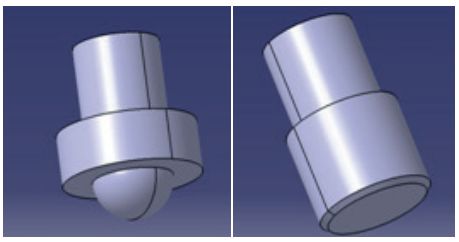

Fig. 4: Geometry of the impactors

4.1. Virtual CAI results

For the sake of brevity, only the results of the tests, carried out on the P80 specimens, with hemispherical impactor, are reported in this work. Nevertheless, results obtained with the Zefiro23 and Zefiro9 specimens, for both hemispherical and flat impactor , were found qualitatively similar to those ones presented below.

In Fig. 5a the damaged area is plotted as function of the impact energy. The damaged area distribution for each type of intralaminar failure is shown in Fig. 5b. The tensile matrix failure mode was found the most relevant one for each energy level. In Fig. 6 the residual strength as function of the impact energy is plotted. The figure shows that once defined the design strain limit at which the component can work (in the picture set equal to 5000 με), it is possible to establish if the component should be repaired or not: the component has to be repaired if, for a given impact energy level, its residual strength is lower than the design strain limit. In the example shown in Fig. 6, the component should be repaired if the impact energy is greater than 30J.

For each stage, the damaged area plotted as function of the impact energy shows a linear trend, with a maximum damaged area at an impact energy of 150 J equal to 4599 mm^2 for P80 (see Fig. 5a), 5322 mm^2 for Zefiro23 and 6611 mm^2 for Zefiro9. However, although the damaged area increases linearly with the increase of the impact energy, the residual strength does not decay linearly, but it attains an asymptotic value equal to 3500 με for P80 (see Fig. 6), 3050 με for Zefiro23 and 2000με for Zefiro9. As matter of the fact, by increasing the impact energy the damaged area extends in such a way to generate a not significant further reduction of the specimen resistant section.

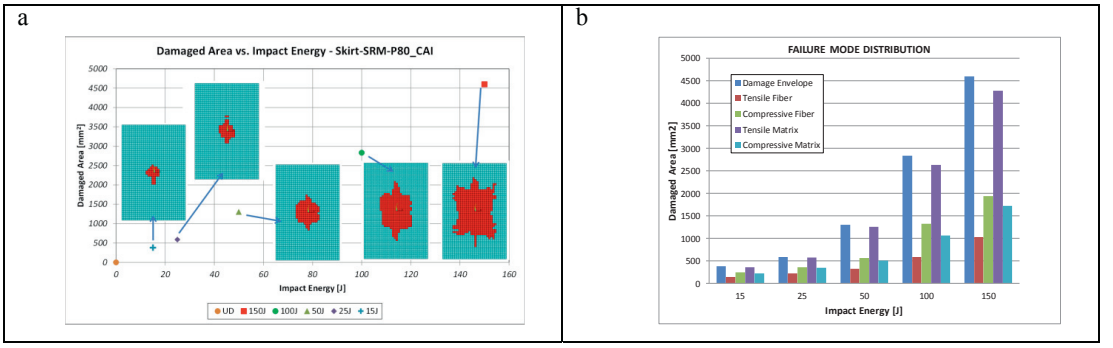

Fig. 5: Skirt SRM P80 – (a) Damaged area vs. impact energy; (b) Damaged area distribution for each type of intralaminar failure

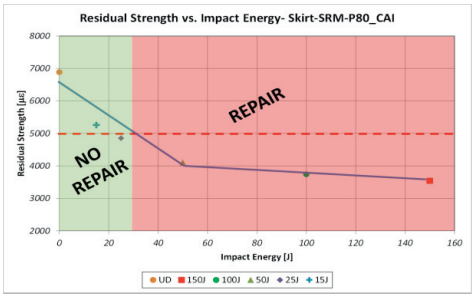

Fig. 6: Skirt SRM P80 – Residual strength vs. impact energy

4.2. Hemyspherical vs. flat impactor

In Fig. 7a a comparison between the total damaged area, obtained with the hemispherical (H) and flat impactor (F) for each energy level and for each stages of the launch vehicle VEGA, is shown: for the same energy level and structural configuration, the flat impactor always produces a damaged area greater than that one obtained with the hemispherical impactor.

The damaged area obtained with the flat impactor is 50% higher than that one induced by the hemispherical impactor for impact energy until to 50J, and only 30% higher for impact energy greater than 50J.
However from Fig. 7b, which shows the compression fiber failure damaged area as function of the impact energy, and Fig. 7c, which shows the tensile fiber failure damaged area as function of the impact energy, it was found that:

- For impact events until to 50J, the hemispherical impactor always produces more extensive damage than that one induced by flat impactor. In particular, for the flat impactor and at these energy levels, the fiber failure was not found.
- For impact events greater than 50J, the hemispherical impactor produces damage generally smaller or in some cases equal to the damage induced by the flat impactor.

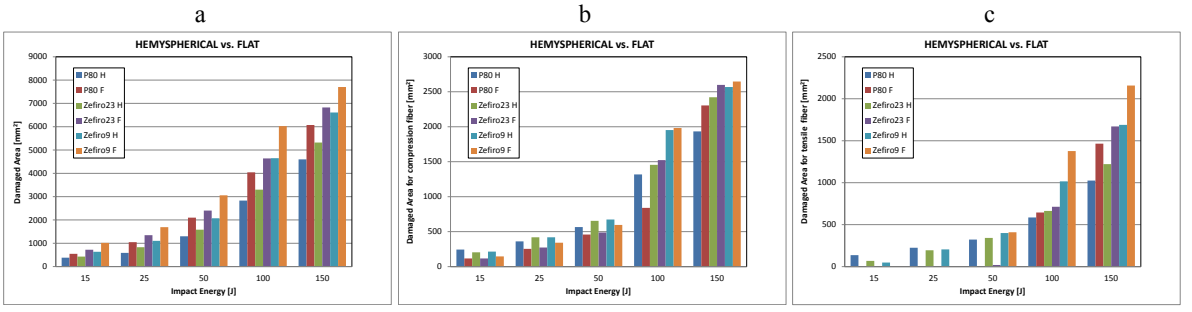

Fig. 7: Damaged area in function of impact energy - Comparison between hemispherical (H) and flat impactor (F) for each stage (a) Total damaged area; (b) Damaged area for compression fiber; (c) Damaged area for tensile fiber.

From Fig. 8, which shows the comparison between the residual strength vs. impact energy curves, obtained with the two types of impactor respectively for P80, Zefiro23 and Zefiro9, it was found that:

- For energy levels until 50J, the residual strength of specimens damaged with flat impactor is greater than the residual strength of specimens damaged with hemispherical impactor. As matter of fact, the compression residual strength is affected by fiber failure and for the specimens impacted at these energy levels, with flat impactor, this failure type does not occur.
- For impact events greater than 50J, significant differences between residual strength in specimens impacted with the two types of impactor were not found.

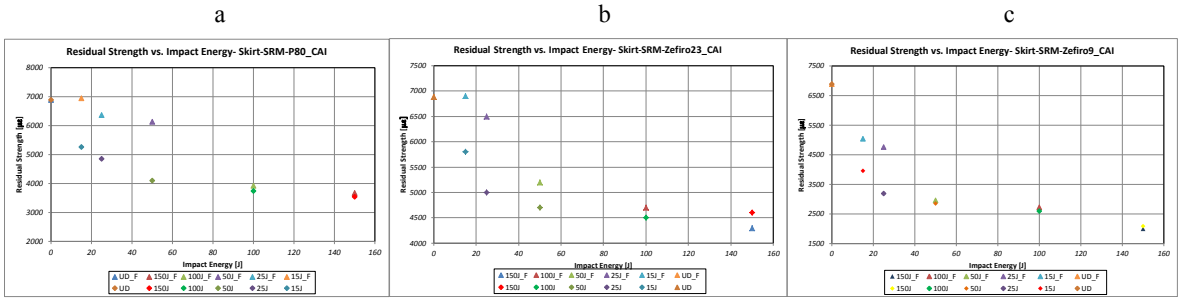

Fig. 8: Residual strength vs. impact energy – Hemispherical (H) vs. flat impactor (F) for each stage (a) P80; (b) Zefiro23; (c) Zefiro9

Acknowledgements

This work was performed in the frame of the project PRADE (PON02_00029_3205863) granted to IMAST S.c.a.r.l. and funded by the MIUR.

References

[1] Abrate, S.: Impact on composite stuctures. Cambridge University Press; 1998.
[2] Abrate, S.: Impact of composite laminates. Appl. Mech. Rev. 44, 155-190 (1991).
[3] Abrate, S.: Impact of composite laminated composites: recent advances. Appl. Mech. Rev. 47, 517-544 (1994).
[4] Reis, L. and de Freitas, M.: Damage growth analysis of low velocity impacted composite panels, Compos. Struct 38, No. 1-4, 509-515 (1997).
[5] de Freitas, M. and Reis, L.: Failure mechanisms on composite specimens subjected to compression after impact, Compos. Struct. 42, 365-373 (1998).
[6] Liu, D., Raju, B.B. and Dang, X.: Size effects on impact response of composite laminates, Int. J. of Imp. Engin. 21(10), 837-854 (1988).
[7] Habib, F.A.: A new method for evaluating the residual compression strength of composites after impact, Compos. Struct. 53, 309-316 (2001).
[8] Cartiè, D.D.R. and Irving, P.E.: Effect of resin and fibre properties on impact and compression after impact performance of CFRP, Compos. Part A 33, 483-493 (2002).
[9] Malhotra, A. and Guild, F.J.: Impact Damage to Composite Laminates: Effect of impact loaction, Appl. Compos. Mater. (2014). doi 10.1007/s10443-013-9382-z
[10] Sanchez-Saez, S., Barbero, E. and Navarro, C.: Compressive residual strength at low temperatures of composite laminates subjected to low velocity impacts, Compos. Structur. 85, 226-232 (2008).
[11] EASA AMC 20-29. Composite Aircraft Structure (2010).
[12] Aoki, Y., Kondo, H. and Hatta: Effect of delamination propagation on mechanical behavior in compression after impact, 16th International Conference on Composite Materials, Kyoto, Japan (2007).
[13] Riccio, A. and Tessitore, N.: Influence of loading conditions on the impact damage resistance of composite panels, Comp. and Struct. 83, 2306-2317 (2005).
[14] Sala, G.: Post-impact behavior of aerospace composites for high-temperature applications: experiments and simulations, Compos. Part B 28B, 651-665 (1997).
[15] Hawyes, V.J., Curtis, P.T. and Soutis, C.: Effect of impact damage on the compressive response of composite laminates, Compos. Part A 32, 1263-1270 (2001).
[16] Soutis, C. and Curtis, P.T.: Prediction of the post-impact compressive strength of CFRP laminated composites, Compos. Science and Techn. 56, 677-684 (1966).
[17] Dang, T.D. and Hallett, S.R.: A numerical study on impact and compression after impact behavior of variable angle tow laminates, Compos. Structur. 96, 194-206 (2013).
[18] Gonzales, E.V., Maimì, P., Camanho, P.P., Turon, A. and Mayugo, J.A.: Simulaztion of drop-weight impact and compression after impact tests on composite laminates, Compos. Structur. 94, 3364-3378 (2012).
[19] Bouvet, C., Rivallant, S. and Hongkarnjanakul, N.: Failure analysis of composite laminate subjected to impact and compression after impact, Workshop Understanding Failure Mechanisms of Composites for Sustaining and Enhancing Military Systems Structures, Riga, Latvia, 7-9 October 2013.
[20] Van den Brink, W.M., Van de Vrie, G. and Nawijn, M.: Post-Impact Residual Strength Analysis of Composite Aerospace Structures using Progressive Damage Methods, Workshop Understanding Failure Mechanisms of Composites for Sustaining and Enhancing Military Systems Structures, Riga, Latvia, 7-9 October 2013.
[21] Borrelli, R., Franchitti, S., Di Caprio, F., Romano, F. and Mercurio, U.: A Numerical procedure for the VIrtual compression after impact analysis, accepted for publication on Applied Composite Materials.
[22] ASTM D7136: American Standard Test Method for measuring the damage resistance of a fiber-reinforced polymer matrix composite to a drop-weight impact.
[23] ASTM D7137: Standard Test Method for Compressive Residual Strength Properties of Damaged Polymer Matrix Composite Plates.
[24] Borrelli, R., Franchitti, S., Di Caprio, F., Mercurio, U., Primavera, V. and Perillo, M.: A CAE Based Procedure to Predict the Low Velocity Impact Response of a Composite CAI Specimen, International CAE Conference 2013, 21-22 October, Verona, Italy.
[25] Chang F.K., Chang K.Y.: “A progressive damage model for laminated composites containing stress concentrations.”, J. of Compos. Mater. 21, 834-855 (1987).
[26] ANSYS® 14.5, Help Manual
[27] Zallo, A., Buono, R., “PRADE PROGRAM - Vega SRMs Evaluation of expected Impact Energy during manufacturing Life Cycles activity”, Internal document NTEPRD10001 Ed.2 (2012)